

Structural and Electronic Properties of Neutral Phosphoniobenzo[*c*]phospholides

Stefan H p,^[a] Laszlo Szarvas,^[a] Martin Nieger,^[a] and Dietrich Gudat^{*[a]}

Keywords: Phosphorus / Phosphorus heterocycles / Electronic structure / Conjugation / Zwitterions

The neutral monophosphoniobenzo[*c*]phospholides **2** and **3** were selectively prepared by reduction of bis(triphenylphosphonio)benzophospholide chloride **1**[Cl]. Compound **3** was further converted into the borane adduct **6** and the thioxo-phosphorane **7**. All products were characterised by spectroscopic methods and X-ray diffraction. The most notable features of the molecular structures are the significantly different distances of the two P–C bonds adjacent to the two-coordinate phosphorus atom (P2–C1 175.0–176.6, P2–C3 171.7–173.5 pm), and a short exocyclic C–P(phosphonio) bond (C1–P1 172.5–173.7 pm) relative to cationic derivatives such as **1**. Structure comparisons revealed further variations in the bond lengths, which can be related to the changes in

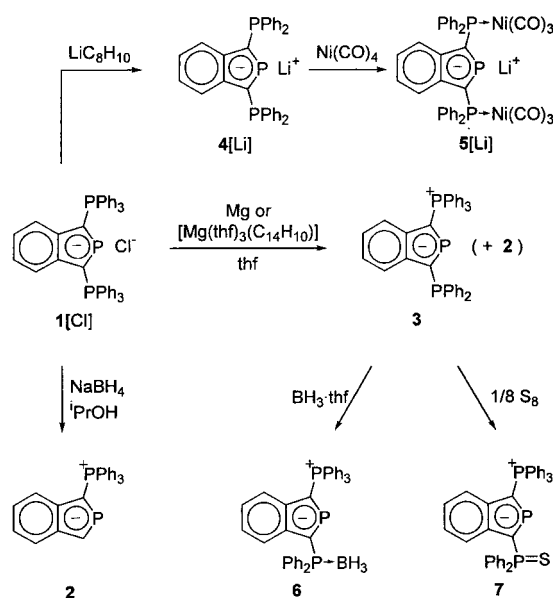
the inductive electron-withdrawing power of the substituents in the 3-position of the fused ring system. Computational studies of monophosphoniobenzo[*c*]phospholides, as well as the corresponding anions with no phosphonio substituents, and cations with two phosphonio substituents, allowed for the interpretation of the special properties of the neutral species in terms of a partial π -bond localisation. This, in terms of a VB picture, is equivalent to the prominence of a single resonance structure that can best be described as an ylide-substituted cyclic phosphalkene. The analysis of these results allows important predictions for the chemical properties of these compounds.

Introduction

Bis(phosphonio)benzo[*c*]phospholide [bis(phosphonio)-2-phosphaindenide] cations such as **1**^[1] exhibit a very special bonding situation that has been described in terms of a benzophospholide anion with a delocalised heteronaphthalenic 10π -electron system, and two positively charged phosphonio substituents.^[2,3] Although electron delocalisation over the phosphonio groups and the π -electron system is low,^[2,4] the electrostatic influence of the substituents still induces a marked reduction in nucleophilicity relative to the anionic phospholide derivatives, and polarises the π -electron distribution in the ring.^[2–4] As a consequence of these effects, bis(phosphonio)benzophospholides display a very balanced nucleophilic and electrophilic reactivity, which is the primary reason for their remarkable stability towards solvolysis and addition reactions,^[1,3,5] and their preference to coordinate to transition metal atoms through the phosphorus lone-pair^[3,6] rather than the π -electron system as most other phospholide-type ligands.^[7]

In the course of the investigation of the chemical properties of bis(phosphonio)benzophospholides, we established that reduction of **1** gives easy access to both neutral, zwitterionic phosphoniobenzo[*c*]phospholides **2**, **3**, and phosphanylbenzophospholide anions **4** (see Scheme 1).^[8] Although a structural study of the carbonylnickel complex **5** revealed that the endocyclic bond lengths and angles are very similar to those of cation **1**,^[8] one can expect that an

increasing electrostatic polarisation by positively charged substituents should induce a concomitant modification of the π -electron distribution in the fused ring system. This view is, in principle, supported by the results of a comparative theoretical study of the parent benzo[*c*]phospholide anion and the corresponding bis(phosphonio)-substituted cation.^[2] However, a concise investigation with regard to this issue is still lacking.



Scheme 1

In the present work we present a combined experimental and computational study of the molecular and electronic structures of the neutral 1-(triphenylphosphonio)enzo[*c*]-

^[a] Anorganisch Chemisches Institut der Universität Bonn, Gerhard-Domagk-Stra e 1, 53121 Bonn, Germany
Fax: (internat.) + 49-(0)228/73-5327
E-mail: dgudat@uni-bonn.de

Supporting information for this article is available on the WWW under <http://www.eurjic-com> or from the author.

phospholides **2** and **3**, the borane adduct **6**, and the thioxophosphorane derivative **7** (Scheme 1). The studied compounds were selected for two main reasons. Firstly, comparison of the bonding situation in **2** and **3** with that in the “symmetrically” substituted ions **1** and **4**, should allow us to see if the polarisation by a *single* charged phosphonio moiety leads to an imbalance in the π -electron distribution, which may result in partial bond localisation. Secondly, comparison of the bonding situation in **3** with that in the borane adduct **6**, thioxophosphorane **7**, and the phosphonium salt **1** should allow for the monitoring of the differential effects which accompany the increasing local positive charge on the phosphorus atom of the substituent in the 3-position. The understanding of both effects is considered important for an improved understanding of the chemical properties of the studied benzo[*c*]phospholide derivatives, and, in particular, of their behaviour in complexation reactions. The latter issue is of special interest in light of the fact that aromatic phosphorus heterocycles have gained recent attention as ligands in catalysis, because of their unusual electronic properties.^[9]

Results and Discussion

Syntheses and Spectroscopic Investigations

3-Diphenylphosphanyl-1-triphenylphosphoniobenzo[*c*]phospholide (**3**) was prepared as described previously,^[8] by reduction of bis(triphenylphosphonio)benzo[*c*]phospholide chloride (**1**[Cl]) with active magnesium, which was generated by the decomposition of $[\text{Mg}(\text{THF})_3(\text{anthracene})]^{[10]}$ in boiling toluene (Scheme 1). Further investigation of this reaction revealed that direct use of Mg/anthracene as a reducing agent gave slightly lower yields of the product, but required less effort for the preparation of the reagent and shorter induction times. 1-Triphenylphosphoniobenzo[*c*]phospholide (**2**) was formed as a by-product in all the reactions, but could not be isolated as it decomposed during the workup procedure. However, the specific formation of compound **2** was observed when the reduction of **1**[Cl] was carried out with NaBH_4 in 2-propanol.^[11] Under these conditions the product precipitated from the reaction mixture. It was easily separated from the formed PPh_3 and borate salts by filtration, and was isolated in good yield after recrystallisation from THF/*i*PrOH.

Having shown that quaternisation of the phosphane functionality in **3** with alkyl halides provides easy access to various side-chain-functionalised bis(phosphonio)benzo[*c*]phospholide cations,^[6] we anticipated that this compound should similarly undergo other typical phosphane reactions such as oxidation or formation of adducts with Lewis acids. In agreement with this assumption, treatment of **2** with equimolar amounts of borane–THF or sulfur afforded quantitative yields (based on ^{31}P NMR spectroscopic investigation of the reaction mixtures) of the corresponding borane adduct **6** and thioxophosphorane **7**, respectively. Use of excess reagents or prolonged reaction times gave no evidence for the quaternisation of the endocyclic phos-

phorus atom, and both products were isolated in good yields after evaporation of the volatiles and recrystallisation from THF/hexane.

The isolated zwitterionic phosphoniobenzo[*c*]phospholides are bright yellow to colourless solids, which are reasonably stable towards air and moisture. All products are readily soluble in polar aprotic solvents (CH_2Cl_2 , MeCN, THF), very sparingly soluble in toluene, and insoluble in hexane.

The purities and identities of all compounds were unequivocally established by analytical and multinuclear (^1H , ^{11}B , ^{13}C , ^{31}P) NMR spectroscopic data. The $^{31}\text{P}\{^1\text{H}\}$ NMR spectra display characteristic AMX (**3**, **6**, **7**) or AX patterns (**2**) (Table 1). The chemical shifts of the exocyclic phosphorus nuclei fall in the expected ranges associated with the different types of functionalities. The resonance of the endocyclic phosphorus atom in **2** appears more upfield than that in **3**, whereas the corresponding resonances in **6**, **7** are more downfield and exhibit similar chemical shifts as the bis(methyldiphenylphosphonio)benzo[*c*]phospholide cation ($\delta^{31}\text{P} = 229.0^{[8]}$). Besides the resonances of the C_6H_5 groups, the ^1H NMR spectra of all the compounds display the expected ABCD patterns for the protons of the benzo[*c*]phospholide moiety. For **2**, the signal assigned to 3-H is buried under other resonances in the aromatic region; however, it can clearly be seen in a two-dimensional ^1H , ^{31}P -HMQC spectrum. The ^1H and ^{11}B NMR spectra of **6** show the expected broad multiplets assigned to the BH_3 moiety. The ^{13}C NMR spectra of all zwitterionic benzophospholides reveal close similarities with those of the bis(phosphonio)-substituted cations.^[1–4,6] However, major differences are observed predominantly for the resonances of the two carbon atoms adjacent to the endocyclic phosphorus atom (cf. Table 1). In comparison with **1**, the signals of the

Table 1. ^{31}P and selected ^{13}C NMR spectroscopic data of zwitterionic phosphoniobenzo[*c*]phospholides; phosphorus atoms are denoted as P1, P2, and P3, and carbon atoms as C1 and C3 in agreement with the numbering scheme given in Figure 1

	$\delta^{31}\text{P}$	$J_{\text{P,P}}$ [Hz]	$\delta^{13}\text{C}$	$J_{\text{P,C}}$ [Hz]
2	190.2 (P2) 15.1 (P1)	87.7	86.4 (C1) 138.3 (C3)	102.8 ($J_{\text{P1,C}}$), 54.8 ($J_{\text{P2,C}}$), 36.8 ($J_{\text{P2,C}}$), 13.5 ($J_{\text{P1,C}}$)
3	218.4 (P2) 14.7 (P1) –21.4 (P3)	82.4 ($J_{\text{P1,P2}}$) 97.2 ($J_{\text{P2,P3}}$)	92.8 (C1) 143.2 (C3)	99.0 ($J_{\text{P1,C}}$), 59.9 ($J_{\text{P2,C}}$), 12.0 ($J_{\text{P3,C}}$), 53.6 ($J_{\text{P2,C}}$), 14.1, 11.9
6	230.8 (P2) 15.5 (P1) 9.4 (P3)	86.1 ($J_{\text{P2,P3}}$) 88.4 ($J_{\text{P1,P2}}$)	98.3 (C1) 144.8 (C3)	98.6 ($J_{\text{P1,C}}$), 58.1 ($J_{\text{P2,C}}$), 11.6 ($J_{\text{P3,C}}$) 11.7, 9.4
7	228.3 (P2) 16.1 (P1) 35.0 (P3)	88.4 ($J_{\text{P2,P3}}$) 88.7 ($J_{\text{P1,P2}}$)	98.4 (C1) 135.7 (C3)	97.5 ($J_{\text{P1,C}}$), 58.8 ($J_{\text{P2,C}}$), 14.1 ($J_{\text{P3,C}}$), 88.1 ($J_{\text{P3,C}}$), 59.1 ($J_{\text{P2,C}}$), 13.2 ($J_{\text{P1,C}}$)

C-1 atoms adjacent to the exocyclic Ph_3P moiety are shifted upfield by about 10–20 ppm and approach the typical values observed for stable phosphonium ylides,^[12] whereas the resonances of the C-3 atoms are deshielded by about 25–35 ppm and are similar to the chemical shifts for phosphinines.^[12] On the whole, although the average chemical shift of both resonances ($\delta = 112.4\text{--}121.5$) changes little relative to that of the cation **1** ($\delta = 109.0$ ^[11]), their large difference provides the first evidence for a marked polarisation of the π -electrons.

The UV/Vis spectra of the neutral benzo[*c*]phospholides display four major absorption bands whose positions and intensities are similar to those of the cation **1**^[13] (Table 2). All observed electronic transitions display the characteristically high extinction coefficients of $\pi\text{--}\pi^*$ transitions and are much stronger than $\pi\text{--}\sigma^*$ transitions which are typical for ylides.^[14] The two bands between 235 and 265 nm are assigned to $\pi\text{--}\pi^*$ transitions within the peripheral phenyl

rings of the Ph_2P and Ph_3P^+ moieties, and the two bands at the lowest wavelengths are assigned to transitions of the benzophospholide chromophore. Absorption bands assigned to $n\text{--}\pi^*$ transitions are not observed and are presumably obscured by the much more intense $\pi\text{--}\pi^*$ transitions. The position of the energetically lowest absorption is comparable with those in 2-phosphanaphthalenes.^[15] Examination

Table 2. UV/Vis data (in CH_2Cl_2) of the zwitterionic phosphoniobenzo[*c*]phospholides **2**, **3**, **6**, **7**, and the salt **1**[Cl] (from ref.^[13])

	λ_{max} [nm] ($\epsilon_{\text{max}}/10^3$ [$\text{l}\cdot\text{mol}^{-1}\cdot\text{cm}^{-1}$])			
1 [Cl]	227 (52)	260 (16)	338 (11)	353 (13)
2	239 (33)	258 (31)	314 (17)	354 (12)
3	236 (47)	251 (45)	330 (sh)	372 (16)
6	241 (45)	263 (26)	334 (11)	359 (13)
7	238 (46)	254 (45)	336 (16)	361 (21)

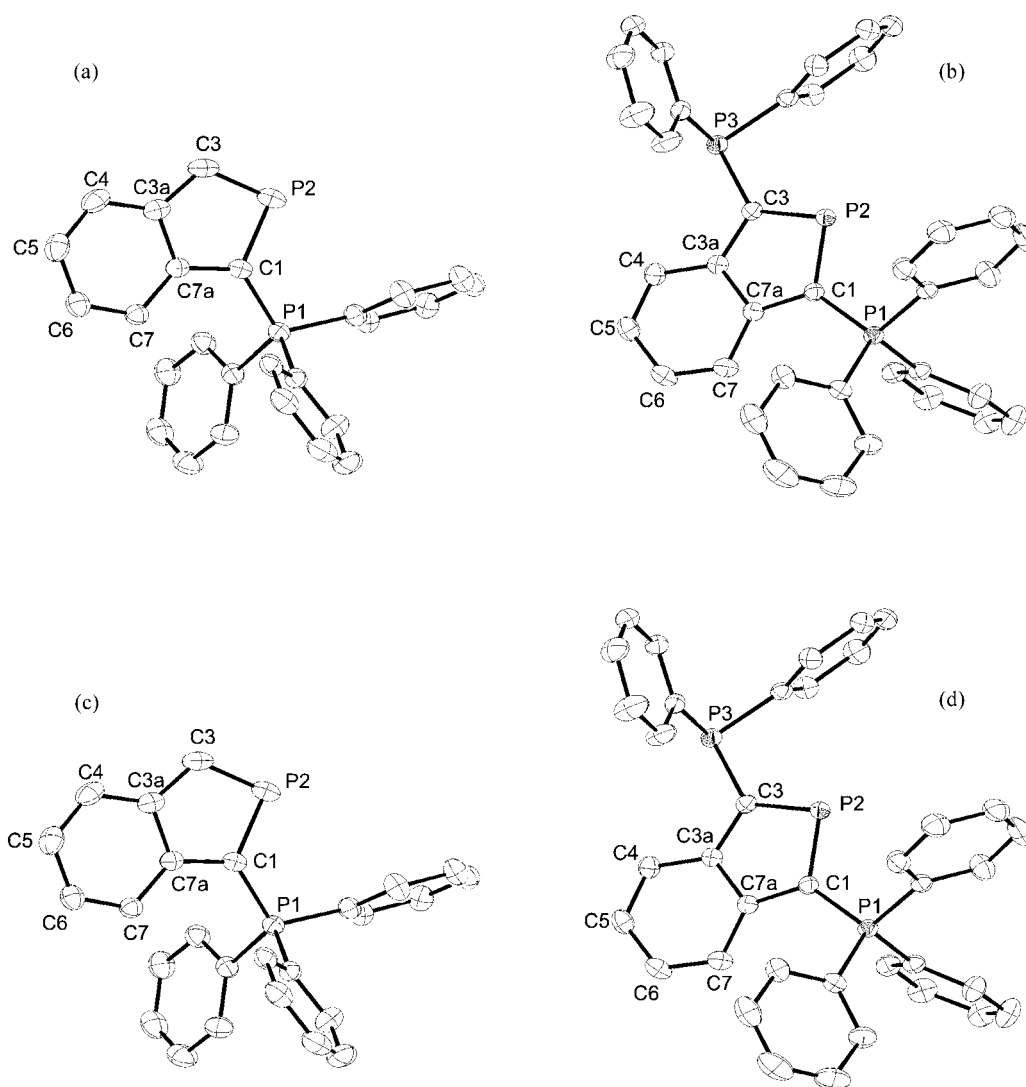


Figure 1. ORTEP-style view of the molecular structures of **2** (a), **3** (b), **6** (c), and **7** (d) with thermal ellipsoids drawn at the 50% level; hydrogen atoms are omitted for clarity, selected bond lengths are given in Table 3; in order to obtain a unique scheme, the crystallographic numbering was changed and a numbering scheme consistent with IUPAC rules used for the ring atoms; exocyclic phosphorus atoms are labelled as P1 (phosphonio group in the 1-position of the ring) and P3 (substituent in the 3-position of the ring)

of the spectra of the 3-substituted neutral compounds **3**, **6**, **7** and the cation **1**, reveals a continuous blue-shift of the energetically lowest absorption band with increasing electron-withdrawing power of the substituent in the 3-position, and an opposite trend for the second lowest absorption band.

Crystal Structure Studies

Suitable single crystals of **2**, **6**, and **7** were grown by slow evaporation of saturated THF solutions. Single crystals of **3** were obtained by cooling a saturated solution in toluene to $-30\text{ }^{\circ}\text{C}$. The molecular structures are shown in Figure 1, and selected bond lengths are given in Table 3. The corresponding data of the cation **1**^[16] and the anionic complex **5**^[8] were included for comparison.

The results of the X-ray structure analyses reveal that the benzophospholide moieties in compounds **2** and **3** are planar, whereas in **6** and **7** the atoms in the benzene unit are slightly twisted around the long axis of the fused ring system. The origin of this distortion presumably arises from crystal packing effects; this effect is not considered significant and therefore will not be discussed further. The exocyclic phosphorus atoms in all compounds are located in the ring planes. The phenyl substituents at the exocyclic P2 and P3 atoms in **3** display a staggered conformation when observed along the P2–P3 axis, and those in **6** and **7** are eclipsed. As in the cation **1**,^[16] the endocyclic phosphorus atom is always confined between two phenyl rings so that the P–B and P–S bonds (in **6** and **7**), or the hypothetical axis of the lone-pair (in **3**) at the exocyclic P3 atom, form angles of approx. $60\text{--}70^{\circ}$ with the ring plane.

The lengths of all C–C bonds in the benzophospholide moiety (136–144 pm) lie in a range which is typical for aromatic systems and match those of corresponding bonds in indoles and indolyl anions.^[17] Endocyclic and exocyclic P–C distances in the zwitterions **2**, **3**, **6** and **7** are similar to those in the ions **1** and **5**,^[8,16] and are intermediate between pure single and double bond lengths. Comparison of the C1–P2 and P2–C3 bond lengths in the same molecule

reveals the former to be significantly longer than the latter in all zwitterions. The effect is largest for **2** [$\Delta r_{\text{P-C}} = 4.9(3)\text{ pm}$] and decreases continuously for **3** [$\Delta r_{\text{P-C}} = 3.3(3)\text{ pm}$] and **6**, **7** [$\Delta r_{\text{P-C}} \approx 1.9(4)\text{ pm}$]. This effect is not observed in **1** and **5**, which have identical substituents at the C1 and C3 atoms, and in “asymmetric” bis(phosphonio)benzophospholides^[6] with two different phosphonio groups. No similar asymmetry of the C–C bonds on opposite sides of the ring system is observed in any compound.

Comparison of corresponding bond lengths and angles in the fused rings of the disubstituted compounds **1**, **3** and **5–7** reveals that the C–C bonds and all bond angles are indistinguishable within experimental error. Insignificant variations were also found for the P2–C3 and the exocyclic P1–C1 bonds, whereas the C1–P2 bond lengths increase slightly but systematically in the series $\mathbf{3} < \mathbf{6} \approx \mathbf{7} < \mathbf{1}$. The endocyclic P2–C3, C1–C7a, and C3–C3a bonds in the monosubstituted zwitterion **2** are shorter than the corresponding bonds in **3** by approx. 1 pm. A similar shortening is also observed for the exocyclic P1–C1 bond, and might suggest a slight increase in the ylidic nature of the phosphonio group. However, it must be noted that although the discussed differences and trends are significant when compared with the estimated standard deviations, it cannot be ruled out that these differences may have arisen from crystal packing effects or other intermolecular interactions (cf. the bond length differences between crystallographically independent molecules of **5** which are of similar magnitude). A further interpretation of these effects is thus, in our opinion, only meaningful when linked with the results of computational studies (see below).

The more pronounced variation of the C3–P3 distances in the studied zwitterions is easily explained in terms of the different substitution patterns at the P3 atom. Both the P3–B bond in **6** [193.15(19) pm] and the P3–S bond in **7** [196.90(7) pm] are longer than those in the corresponding triphenylphosphane derivatives (P–B in $\text{Ph}_3\text{P-BH}_3$ 190.1 pm,^[18] P–S in $\text{Ph}_3\text{P=S}$ 195.2 pm^[19]), and lie near the upper limit of the known expected ranges for borane adducts and

Table 3. Selected bond lengths [pm] in the zwitterionic phosphoniobenzophospholides **2**, **3**, **6**, **7**, the cation of the salt **1**[CpW(CO)₃] (data taken from ref.^[16]), and the anion of the salt **5**[Li(THF)₄] (data taken from ref.^[8]); the atom numbering scheme is identical to the one given in Figure 1

	1	2	3	5 ^[a]	6	7
C1–P2	172.8(4)	176.62(11)	176.23(13)	173.2(4) 174.7(4)	174.99(17)	175.40(19)
P2–C3	172.9(4)	171.71(14)	172.93(12)	1.736(4) 174.4(4)	173.23(16)	173.53(19)
C3–C3a	144.1(6)	142.09(17)	143.38(18)	144.0(5) 143.1(5)	143.6(2)	143.7(3)
C3a–C4	140.2(6)	141.46(18)	141.82(17)	141.3(5) 140.0(5)	141.0(2)	141.4(3)
C4–C5	136.3(7)	137.7(2)	137.56(19)	137.2(5) 138.0(5)	136.9(2)	137.0(3)
C5–C6	139.1(8)	140.36(18)	140.7(2)	139.9(6) 140.1(5)	140.2(2)	140.0(3)
C6–C7	138.0(8)	137.51(16)	137.66(19)	136.7(5) 137.1(5)	137.7(2)	137.4(3)
C7–C7a	139.8(6)	141.26(15)	141.58(18)	141.6(5) 141.6(5)	141.5(2)	141.0(3)
C7a–C1	144.9(6)	142.95(15)	143.93(17)	144.1(5) 142.3(5)	143.7(2)	143.7(3)
C3a–C7a	142.3(6)	143.02(15)	143.06(17)	143.2(5) 144.0(5)	143.0(2)	142.5(3)
P1–C1	174.7(4)	172.55(11)	173.47(12)	178.9(4) 177.7(4)	173.51(16)	173.65(19)
P3–C3	174.9(4)	–	180.92(13)	178.0(4) 177.4(4)	178.24(16)	177.42(19)

^[a] The given values refer to two crystallographically independent molecules per unit cell.

sulfides of tertiary phosphanes (P–B 192.2 ± 2.7 , P–S 195.4 ± 0.5 pm^[17]). This suggests a comparatively low nucleophilicity of the exocyclic phosphane moiety in the studied molecules.

Computational Studies

In order to carry out a meaningful discussion of the changes in structure and bonding in the studied phosphoniobenzophospholides, and to gain a reliable basis for the interpretation of rather small structural distortions, we performed a comprehensive computational study using the B3LYP density functional method,^[20] employed in the GAUSSIAN 98^[21] suite of programs. To minimise computation times, the calculations were performed on the model compounds **1-H**–**4-H**, **6-H**, **7-H**, in which all peripheral phenyl rings of **1**–**4**, **6**, **7** had been replaced by hydrogen atoms, and any interaction of ionic species with the appropriate counter-ion was neglected.^[22] The molecular structures of all compounds were obtained from energy optimisations at the B3LYP/6-31+g* level, and were shown to be local minima on the energy hypersurface by means of vibrational analyses. The results revealed that in the most stable conformers of compounds **3-H**, **6-H**, and **7-H**, the P–X axes of the PH₂X units (X = BH₃, S, lone-pair) form an angle of approx. 60° with the ring plane. This is in agreement with the experimentally observed conformations of **3**, **6**, **7** and implies a molecular C₁ symmetry. The molecular structures of **1-H** and **4-H** display C_{2v} symmetry, in agreement with the results of earlier computational studies of **1-H** at a different theoretical level,^[2] and with the experimentally observed conformations of **1**^[16] and complex **5**.^[8] As the molecular structures of **3-H**, **6-H**, **5-H**, and **7-H** allow no clear-cut separation between orbitals of σ- and π-symmetry, we re-optimised the structures of these species under the constraint of C_s symmetry. The resulting molecular structures are local minima on the energy hypersurface whose energies (at the B3LYP/6-31+g* + ZPE level, see Table 4) and metric parameters (apart from the different torsion angles of the PH₂X groups) do not differ significantly from those of the C₁-symmetric conformers. Relevant structural parameters of the “symmetric” (C_s or C_{2v}) conformers, together with π-orbital populations and Wiberg bond indices (WBI), which were computed from NBO population analyses,^[23] are given in Figure 2.^[24] For further discussion we will refer only to the properties of the “symmetric” conformers.

Comparison of the computed bond lengths in the model compounds with the experimental data of **1**–**3**, **6**, and **7** shows a close agreement for all endocyclic C–C bonds and P1–C9 bonds (using the same numbering scheme as in Figure 1). The differences in the bond lengths are less than 1 pm. The computed lengths of the endocyclic C1–P2 bonds are generally about 3 pm longer than the experimental values, and those of the exocyclic C1–P1 bonds are shorter by the same amount. However, the variation of the individual computed bond lengths in different molecules reproduces the same trends that have been found in the experimental studies. This finding strongly suggests that the small

Table 4. Computed absolute energies (at the B3LYP/6-31+g* level), zero-point energies, molecular point groups, and relative energies of different conformers (at the B3LYP/6-31+g* + zpe level) for the model compounds **1-H**–**4-H**, **5-H**, **6-H**

	<i>E</i> [a.u.]	ZPE [kJ/mol]	Symmetry	<i>E</i> ^{rel} [kJ/mol]
1-H	–1334.6269	396.7	C _{2v}	0.0
2-H	–992.3217	344.6	C _s	0.0
3-H	–1334.2684	366.4	C _s	0.0
	–1334.2677	365.7	C ₁	–1.1
4-H	–1333.7776	336.4	C _{2v}	0.0
	–1333.7735	335.2	C ₂	9.7
6-H	–1360.9254	450.2	C _s	0.0
	–1360.9245	450.1	C ₁	–0.2
7-H	–1732.4745	375.5	C _s	0.0
	–1732.4757	376.0	C ₁	2.7

structural variations detected reflect real differences in the electronic structures, rather than being a result of intermolecular interactions in the crystal.

The results of NBO population analyses (cf. Figure 2b) reveal that the total π-electron population in the atoms of the annulated rings (9.75–9.86 electrons) is close to the theoretical value of 10 in all compounds. The small electron loss is attributed to weak hyperconjugation with antibonding P–H orbitals in the peripheral substituents (see below), and is almost independent of the substituent pattern. Inspection of individual atomic π-orbital population indicates a shift of π-electron density from the P2 phosphorus atoms and the remote C5/C6 carbon atoms in the six-membered ring, towards the C1/C3 carbon atoms. This shift increases with the total positive charge and, for **2-H**, **3-H**, **5-H**, and **6-H**, with the electron-withdrawing capability of the substituent on C3. In the neutral compounds, the π-electron density accumulates predominantly at the C1 atom adjacent to the strongly electron-withdrawing PH₃⁺ moiety, thus introducing further pronounced “asymmetry” in the π-electron distribution. This effect is weakened in the series **2-H** > **3-H** > **5-H** ≈ **6-H**, by the growing electron-withdrawing effect of the C-9 substituents.

Inspection of the Wiberg bond indices reveals that the bond orders in the six-membered ring are essentially independent of the substituents in the 1- and 3-positions (Figure 2c). Beginning with the symmetrically substituted ions, both the C1–P2/P2–C3 and the C1–C7a/C3–C3a bond orders in the five-membered ring of the anion **4-H** are higher than those in the cation **1-H**, whereas the opposite trend is found for the C3a–C3a bonds. Interestingly, these variations result in appropriate changes in bond lengths only in the case of the C–C bonds; presumably, lower covalent P–C bond orders in **1-H** are counterbalanced by a larger electrostatic polarisation. For the betaines **2-H**, **3-H**, **6-H**, and **7-H**, the uneven distribution of π-electrons between C1 and C3 coincides with a concomitant polarisation of the P–C bond orders. The P2–C3 bonds display WBIs between 1.37 and 1.49, which are in the range between those of phosphinine (1.38) and methylenephosphane (1.94), and indicate pronounced double-bond char-

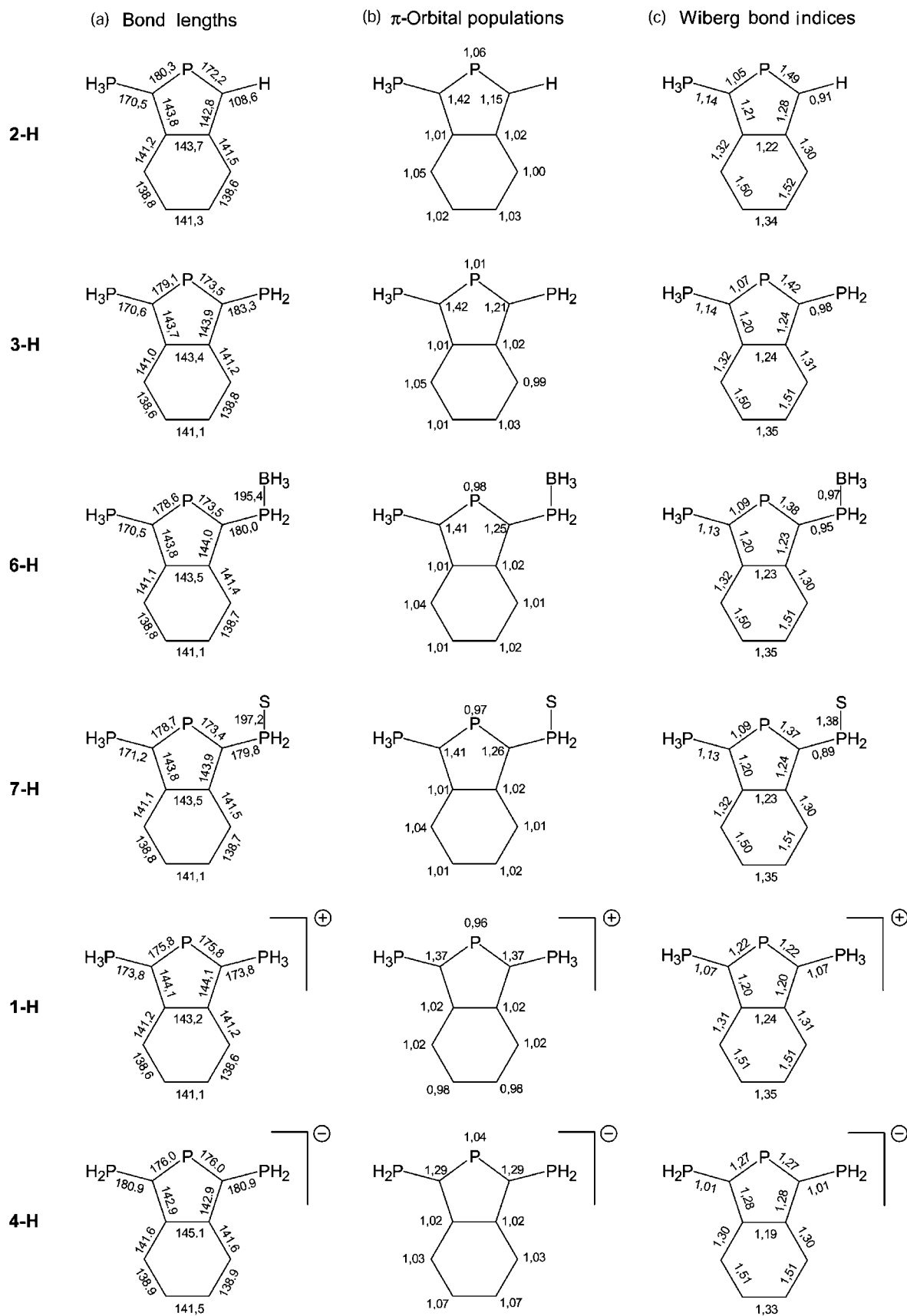
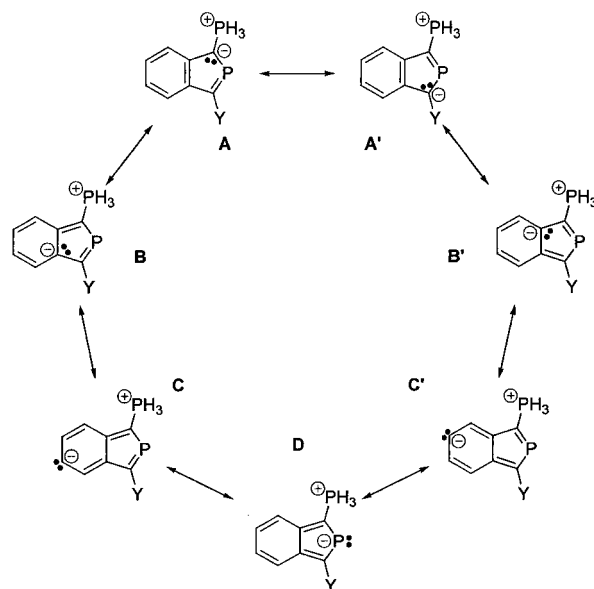


Figure 2. (a) Computed bond lengths, (b) π -orbital populations, and (c) Wiberg bond indices for the model compounds **1-H–4-H**, **5-H**, **6-H**; distances were obtained from energy-optimised molecular structures computed at the B3LYP/6-31+g* level, and orbital populations and bond indices from NBO population analyses^[23] at the B3LYP/6-31 g*/B3LYP/6-31+g* level of theory

acter. The adjacent C1–P2 bonds display lower bond orders (WBI = 1.05–1.09), whose values nonetheless still exceed those of pure single bonds (cf. 0.98–1.01 for the exocyclic C3–P3 bonds in **2-H** and **4-H**). A less pronounced weakening of the bond (see Figure 2c) is also noted for the C1–C7a bond as compared with the C3–C3a bonds. The differences in the bond indices within each pair of P–C and C–C bonds in a single compound decreases slightly with increasing electron-withdrawing character of the substituent at C3. The higher WBIs for the exocyclic C1–P1(phosphonio) bonds in betaines (**1-H**) relative to the symmetrical ions **1-H** (1.07) and **4-H** (1.01), suggest a more pronounced ylide character of this bond. The exocyclic C3–P3 bonds (WBI = 0.89–0.98) are single bonds.

In the frame of a VB picture, a consistent interpretation of the changes in the bonding situation in the studied benzophospholide systems can be given in terms of a superposition of the canonical structures shown in Scheme 2. The results of the NBO analyses suggest that the dominating resonance structures in the cation **1-H** are **A**, **A'**, whose weightings are equal due to symmetry reasons.^[2] For the betaines **2-H**, **3-H**, **6-H**, and **7-H**, the dominant canonical structure is **A**, even though the results of the perturbational analysis of the Fock matrix and the residual delocalisation of NLMOs suggest that the contribution of **A'** increases slightly with the growing electron-withdrawing capability of the substituent **Y**. The contribution of the canonical structure **B** is greater in these compounds than in the cation **1-H**. For the anion **4-H**, the NBO analysis suggests that the contribution of resonance structures **A**, **A'** (with H₂P instead of H₃P⁺) decreases relative to that of the remaining alternatives **B–D**. This effect reflects a more efficient π -delocalisation along the ring perimeter and a shift of the excess charge in the π -system towards the P2 and C5, C6 atoms. The dominance of the 1,2-dipolar canonical structures **A** (and **A'**) in the phosphonio-substituted species can be understood since the charge separation is smallest. It also emphasises the fact that the shift in π -electron distributions between species with different overall charge can be understood mainly by electrostatics as the charges are in close proximity to each other.^[25]

In light of the discussed results it can be concluded that all studied benzophospholides may be described as delocalised 10 π -electron systems, which formally involve the interaction of a benzene (6 π) and a phosphaaallylic (4 π) fragment.^[2] The conjugation between both units (as expressed by increasing contributions of the canonical structures **B–C'** in Scheme 2) increases when the sum of the positive charges on the substituents decreases, and is thus most pronounced in the genuine anion **4-H**. Furthermore, substitution by a single positively charged substituent at the C2 atom in **2-H**, **3-H**, **6-H**, **7-H** lifts the degeneracy between canonical structures **A** and **A'**. The resulting essentially single resonance structure (**A**) brings a “phosphaalkene–benzylidene ylide” structure to the fore, and is equivalent to a partial π -electron localisation.



Scheme 2

With regard to the recent interest in the use of benzophospholide systems as ligands,^[3,6,11] a short account of the nature and energies of frontier orbitals is of interest; this should allow some predictions on the coordination behaviour of these compounds to be made. The energies of selected molecular orbitals are listed in Table 5. As in the cation **1-H**, both HOMOs and LUMOs in the betaines **2-H**, **3-H**, **6-H**, and **7-H** have a'' symmetry, and can be described as the 5 π and 6 π^* orbitals of a heteronaphthalenic 10 π -electron system.^[2] The highest a'-type orbital in **2-H** and **6-H** lies approx. 2 eV below the HOMO and is assigned to a non-bonding pair of electrons centred at the endocyclic P1 phosphorus atom. In **3-H** and **7-H**, this orbital is best described as a “lone-pair” centred at the exocyclic P3 phosphorus or sulfur atoms, respectively. The energies of the phosphorus “lone-pair” orbitals in **2-H** and **6-H** (–7.3 to –7.5 eV) are similar to those calculated for phosphinine (–7.3 eV) or PH₃ (–7.5 eV) at the same level of theory. As expected, the energies of both occupied and unoccupied orbitals are stabilised with increasing overall positive charge of the system, but the HOMO–LUMO gap in all compounds remains essentially unchanged. Even if this finding allows a qualitative rationalisation of the observed similarity of the lowest π – π^* -transition energies, a more detailed interpretation of the electronic spectra is not feasible in the frame of this simple one-electron model. Based on the computed orbital energies it can be predicted that the donor capability of benzo[*c*]phospholide ligands will decrease and their π -acceptor capability will increase with the number of positively charged phosphonio groups, whereas further modifications within the substituents will play a minor role. Furthermore, coordination of a transition metal via a phosphorus lone-pair in **3-H** and **4-H** should take place at the exocyclic three-coordinate rather than the endocyclic two-coordinate phosphorus atom, which is in agreement with

Table 5. Computed energies [eV] and symmetry descriptors (in parentheses) for selected orbitals (at B3LYP/6-31+g* level, see ref.^[24]) and their differences in the “symmetric” conformers of **1-H**–**7-H**

	1-H (C_{2v})	2-H (C_s)	3-H (C_s)	4-H (C_{2v})	6-H (C_s)	7-H (C_s)
$\varepsilon(\text{LUMO})$	−5.34 (b_1)	−1.15 (a'')	−1.40 (a'')	2.45 (b_1)	−1.76 (a'')	−1.76 (a'')
$\varepsilon(\text{HOMO})$	−9.37 (a_2)	−5.26 (a'')	−5.47 (a'')	−1.47 (a_2)	−5.87 (a'')	−5.74 (a'')
$\varepsilon(\text{HOMO} - 1)$	−9.51 (b_1)	−5.63 (a'')	−5.80 (a'')	−1.92 (b_1)	−6.15 (a'')	−5.95 (a'')
$\varepsilon(\text{l.p.})^{[a]}$	−11.54 (a_1)	−7.31 (a')	−6.66 (a') ^[b]	−3.27 (a_1) ^[c]	−7.50 (a'')	−5.88 (a') ^[d]
$\varepsilon(\text{LUMO}) - \varepsilon(\text{HOMO})$	4.03	4.12	4.07	3.92	4.11	3.98

^[a] Highest orbital of a_1 (a') symmetry. — ^[b] Assignment to non-bonding orbital centred at P-3. — ^[c] Symmetric linear combination of non-bonding orbitals centred at all three phosphorus atoms. — ^[d] Assignment to non-bonding orbital centred at S.

the observed formation of the nickel complex **5** starting from **4**.^[8]

Conclusion

Our experimental and computational investigations have shown that the π -electron structures of neutral monophosphoniobenzo[*c*]phospholides are closely related to those of both bis(phosphonio)-substituted cations and genuine benzo[*c*]phospholide anions. However, on the other hand they have also highlighted characteristic deviations, which can be associated with the effects of π -electron polarisation by the charged phosphonio groups. Two major trends emerge from the results: (a) an increasing number of phosphonio substituents in the five-membered ring reduces π -conjugation between the fused rings; (b) a single phosphonio substituent in the 1-position of the fused ring system acts as a π -electron “trap” and induces a strong concentration of π -electron density on the adjacent ring carbon atom, and a concomitant π -bond localisation. Differential tuning of this effect is achieved by varying the inductive electron-withdrawing power of a substituent in the 3-position. With regard to the concomitant increase in ylidic character of the P(phosphonio)–C bond, the π -bond localisation brings a phosphaaalkene ylide type of structure to the fore, which is most pronounced in **2**. Interestingly, a careful comparison of the computational results revealed that the observed variations in the bonding situation were only in part reflected in appropriate structural changes, thus emphasising that great care has to be taken during attempts to interpret the bonding situation exclusively on the basis of structural parameters.

The computational results further allow a number of predictions on the chemical properties of phosphoniobenzo-phospholides to be made. A comparison of frontier orbital energies suggests that the neutral species should behave as better σ/π -donors and weaker π -acceptors than cation **1**, which is in agreement with the conclusions drawn from a recent preliminary study of the complex chemistry of **2**.^[11] In contrast to **2**, which binds a $\text{Cr}(\text{CO})_5$ fragment via the endocyclic two-coordinate phosphorus atom,^[11] complexation of **3** to a 16e-metal complex fragment is expected to occur at the exocyclic phosphane moiety, as in the anion

4.^[8] More importantly, the π -bond localisation in neutral phosphoniobenzo-phospholides towards a phosphaaalkene–benzylidene ylide electronic structure, suggests that these compounds should also display an increased susceptibility towards addition [such as addition of reactive E–H bonds which have been found to occur for less reactive bis(phosphonio)-substituted cations^[5]], or even cycloaddition reactions at the P–C double bond, or Wittig reactions at the ylide moiety. Investigations aiming at the verification of these reaction schemes for **2**, where the largest degree of π -bond localisation is observed, are currently in progress.

Experimental Section

General Remarks: NMR spectra were recorded at 30 °C with a Bruker AMX 300 spectrometer (300.13, 121.50, 96.3 and 75.46 MHz for ^1H , ^{31}P , ^{11}B and ^{13}C). Chemical shifts are referred to external TMS (^1H , ^{13}C), $\text{Et}_2\text{O}\cdot\text{BF}_3$ or 85% H_3PO_4 . The atoms of the benzophospholide moiety are denoted C-1 to C-7a, 4-H to 7-H, and P-1 to P-3, using the numbering scheme given in Figure 1; carbon atoms of the phenyl groups by C_{para} , C_{meta} etc. — UV/Vis spectra: Kontron Uvikon 860. — FAB-MS: Kratos Concept 1 H, Xe-FAB. — Elemental analysis: Heraeus CHNO-Rapid.

3-(Diphenylphosphanyl)-1-(triphenylphosphonio)benzo[*c*]phospholide (3): 1,3-Bis(triphenylphosphonio)benzo[*c*]phospholide chloride (**1**[Cl]) (8.6 g, 12.5 mmol) and magnesium/anthracene·3THF (10.0 g, 24 mmol) were suspended in 50 mL of THF. The mixture was stirred for 8 h, filtered, and water-saturated Et_2O was added to the dark red solution until it turned yellow-orange. The mixture was filtered once more, the filtrate concentrated to dryness, and the orange residue suspended in a mixture of 20 mL of dry Et_2O and 50 mL of DME. Addition of 50 mL of MeOH gave the crude product as a yellow solid. Residual anthracene was removed by extraction with boiling hexane, and recrystallisation from DME/MeOH finally afforded 1.5 g (47%) of **2**, m.p. 179 °C. — Analytical and spectroscopic data are identical to those published in ref.^[8]

1-(Triphenylphosphonio)benzo[*c*]phospholide (2): Solid NaBH_4 (2.5 g, 66 mmol) was added to a stirred suspension of **1**[Cl] (13.75 g, 19.9 mmol) in 150 mL of 2-propanol. It was stirred for 12 h until no starting material (^{31}P NMR control) was left. The mixture was then filtered, the precipitate washed three times with 2-propanol, and the filtrate concentrated to dryness. The yellow solid residue was extracted with 100 mL of THF and insoluble NaBH_4 was filtered off. After concentration of the filtrate in vacuum to a total

volume of 30–40 mL, 2-propanol was added until the precipitation of solid material started (approx. 20–30 mL). Cooling of the solution to 4 °C gave bright yellow crystals of **3**; yield 4.94 g (63%). – ¹H NMR (CDCl₃): δ = 6.71–7.63 (m, 4 H, 4-H to 7-H), 7.42–7.84 (m, 15 H, C₆H₅), 8.20 (dd, ²J_{H,P-2} = 42.3 Hz, ⁴J_{H,P-1} = 6.6 Hz, 1 H, 3-H). – ¹³C{¹H} NMR (CDCl₃): δ = 86.4 (dd, ¹J_{P-2,C} = 54.8 Hz, ¹J_{P-1,C} = 102.8 Hz, C-1), 118.1 (d, ¹J_{P,C} = 0.9 Hz, C-6/5), 119.1 (d, ¹J_{P,C} = 3.9 Hz, C-5/6), 119.6 (d, ¹J_{P,C} = 4.1 Hz, C-7/4), 121.3 (dd, ¹J_{P,C} = 9.0, 1.1 Hz, C-4/7), 125.6 (dd, ¹J_{P-1,C} = 89.5 Hz, ³J_{P-2,C} = 2.2 Hz, C_{ipso}), 129.5 (d, ³J_{P-1,C} = 12.3 Hz, C_{meta}), 133.9 (dd, ²J_{P-1,C} = 10.2 Hz, ⁴J_{P-2,C} = 1.4 Hz, C_{ortho}), 134.6 (d, ⁴J_{P-1,C} = 2.9 Hz, C_{para}), 138.3 (dd, ¹J_{P-2,C} = 36.8 Hz, ³J_{P-1,C} = 13.5 Hz, C-3), 142.4 (dd, ¹J_{P,C} = 9.5, 2.0 Hz, C-3/3a), 145.2 (dd, ¹J_{P,C} = 17.6, 9.5 Hz, C-3/3a). – FAB-MS: *m/z* (%) = 394 (100) [M]⁺ – C₂₆H₂₀P₂ (394.39): calcd. C 79.18, H 5.11; found C 78.17, H 5.88.

3-[(Diphenylphosphanyl)borane]-1-(triphenylphosphonio)benzo[c]-phospholide (6): Compound **2** (0.4 g, 0.69 mmol) was dissolved in 10 mL of THF. After 0.7 mL of a 1 M solution of BH₃·THF in THF had been added, the mixture was stirred for 10 min and then concentrated to dryness. The yellowish residue was recrystallised from THF/hexane; yield 0.41 g (100%), m.p. 227 °C. – ¹H NMR (CDCl₃): δ = 6.70–7.00 (m, 4 H, 4-H to 7-H), 7.20–8.50 (m, 25 H, C₆H₅). – ¹¹B{¹H} NMR (CDCl₃): δ = –28.5 (s, broad). – ¹³C{¹H} NMR (CDCl₃): δ = 98.3 (ddd, ¹J_{P-2,C} = 58.1 Hz, ¹J_{P-1,C} = 98.6 Hz, ³J_{P-3,C} = 11.6 Hz, C-1), 119.5 (s, C-6/5), 120.1 (s, C-5/6), 120.7 (d, ¹J_{P,C} = 3.8 Hz, C-7/4), 122.4 (d, ¹J_{P,C} = 3.9 Hz, C-4/7), 124.8 [d, ¹J_{P-1,C} = 89.8 Hz, C_{ipso}(PPh₃)], 128.6 [d, ³J_{P-3,C} = 9.9 Hz, C_{meta}(PPh₂)], 129.7 [d, ³J_{P-1,C} = 12.4 Hz, C_{meta}(PPh₃)], 130.5 [d, ⁴J_{P-3,C} = 1.9 Hz, C_{para}(PPh₂)], 132.7 [d, ¹J_{P-3,C} = 4.4 Hz, C_{ipso}(PPh₂)], 133.4 [d, ²J_{P-3,C} = 9.5 Hz, C_{ortho}(PPh₂)], 133.7 [d, ⁴J_{P-1,C} = 2.7 Hz, C_{para}(PPh₃)], 134.4 [d, ²J_{P-1,C} = 10.3 Hz,

C_{ortho}(PPh₃)], 144.8 (dd, ¹J_{P-3,C} = 9.4 Hz, ¹J_{P-2,C} = 11.7 Hz, C-3), 145.6 (m, C-3a/7a). – FAB-MS: *m/z* (%) = 592 (20) [M]⁺, 578 (100) [M – BH₃]⁺ – C₃₈H₃₂BP₃ (592.40): calcd. C 77.05, H 5.44; found C 78.07, H 5.24.

3-(Diphenylthioxophosphoranyl)-1-(triphenylphosphonio)benzo[c]-phospholide (7): Compound **2** (0.5 g, 0.86 mmol) and sulphur (30 mg, 0.94 mmol) were dissolved in 10 mL of THF, and the resulting solution was stirred for 12 h. Subsequent addition of 20 mL of hexane produced a precipitate which was collected by filtration, washed with 5 mL of Et₂O/hexane (1:1), and dried in vacuum to give 0.46 g (87%) of a colourless solid, m.p. > 280 °C. – ¹H NMR (CDCl₃): δ = 6.70–6.93 (m, 4 H, 4-H to 7-H), 7.25–7.97 (m, 25 H, C₆H₅). – ¹³C{¹H} NMR (CDCl₃): δ = 98.4 (ddd, ¹J_{P-2,C} = 58.8 Hz, ¹J_{P-1,C} = 97.5 Hz, ³J_{P-3,C} = 14.1 Hz, C-1), 119.8 (s, C-6/5), 120.3 (d, ¹J_{P,C} = 1.7 Hz, C-5/6), 120.5 (d, ¹J_{P,C} = 3.6 Hz, C-7/4), 122.8 (d, ¹J_{P,C} = 4.4 Hz, C-4/7), 124.7 [d, ¹J_{P-1,C} = 89.7 Hz, C_{ipso}(PPh₃)], 128.3 [d, ³J_{P-3,C} = 12.4 Hz, C_{meta}(PPh₂)], 129.6 [d, ³J_{P-1,C} = 12.4 Hz, C_{meta}(PPh₃)], 130.8 [d, ⁴J_{P-3,C} = 2.9 Hz, C_{para}(PPh₂)], 132.8 [d, ²J_{P-3,C} = 10.1 Hz, C_{ortho}(PPh₂)], 133.6 [d, ⁴J_{P-1,C} = 2.9 Hz, C_{para}(PPh₃)], 135.7 (ddd, ¹J_{P-2,C} = 59.1 Hz, ³J_{P-1,C} = 13.2 Hz, ¹J_{P-3,C} = 88.1 Hz, C-3), 134.5 [d, ²J_{P-1,C} = 10.3 Hz, C_{ortho}(PPh₃)], 136.3 [d, ¹J_{P-3,C} = 85.5 Hz, C_{ipso}(PPh₂)], 144.7 (m, C-3a/7a). – FAB-MS: *m/z* (%) = 611 (100) [M]⁺ – C₃₈H₂₉P₃S (610.63): calcd. C 74.75, H 4.79 S 5.25; found C 74.12, H 5.00 S 5.16.

Computational Studies: DFT calculations (B3LYP^[20]) were carried out using the Gaussian 98 program package^[21] with a 6-31 g* basis set which was augmented by one diffuse function for all ring atoms and the exocyclic halogen atoms [6-31(+)*] as implemented in the Gaussian package]. Harmonic vibrational frequencies and zero-

Table 6. Crystallographic data, and details for the structure solution and refinement of **2**, **3**, **6**, **7**

	2	3	6	7
Empirical formula	C ₂₆ H ₂₀ P ₂	C ₃₈ H ₂₉ P ₃	C ₃₈ H ₃₂ BP ₃	C ₃₈ H ₂₉ P ₃ S
<i>M_r</i>	394.4	578.5	592.4	610.6
Crystal dimensions [mm]	0.50 × 0.30 × 0.25	0.30 × 0.25 × 0.20	0.35 × 0.30 × 0.25	0.25 × 0.10 × 0.05
Crystal system	monoclinic	triclinic	monoclinic	monoclinic
Space group	<i>P</i> 2 ₁ / <i>n</i> (No. 14)	<i>P</i> 1̄ (No. 2)	<i>P</i> 2 ₁ / <i>n</i> (No. 14)	<i>P</i> 2 ₁ / <i>n</i> (No. 14)
<i>a</i> [Å]	10.6443(2)	9.2453(2)	10.6833(4)	10.4063(3)
<i>b</i> [Å]	15.0593(3)	11.6227(3)	18.7364(7)	18.7623(6)
<i>c</i> [Å]	12.8699(2)	14.7589(3)	16.2374(8)	16.1564(5)
α [°]	90	84.819(2)	90	90
β [°]	91.498(1)	89.160(2)	102.224(2)	98.960(2)
γ [°]	90	69.255(2)	90	90
<i>V</i> [Å ³]	2062.28(6)	1476.79(6)	3176.5(2)	3115.98(17)
<i>Z</i>	4	2	4	4
ρ [g·cm ^{–3}]	1.27	1.30	1.24	1.30
μ [mm ^{–1}]	0.22	0.23	0.21	0.29
<i>F</i> (000)	824	604	1240	1272
2θ _{max} [°]	56.6	56.6	50.0	50.0
	–13 ≤ <i>h</i> ≤ 13	–12 ≤ <i>h</i> ≤ 12	–12 ≤ <i>h</i> ≤ 12	–12 ≤ <i>h</i> ≤ 12
	–20 ≤ <i>k</i> ≤ 20	–15 ≤ <i>k</i> ≤ 15	–22 ≤ <i>k</i> ≤ 17	–22 ≤ <i>k</i> ≤ 22
	–17 ≤ <i>l</i> ≤ 17	–19 ≤ <i>l</i> ≤ 19	–19 ≤ <i>l</i> ≤ 16	–19 ≤ <i>l</i> ≤ 19
No. of measured data	60523	30935	20057	46091
No. of unique data	5092	7088	5590	5482
<i>R</i> _{int}	0.030	0.032	0.037	0.059
Absorption correction	none	none	none	none
No. parameters/restraints	253/0	370/0	381/0	379/0
<i>R</i> [for <i>I</i> > 2 σ(<i>I</i>)]	0.032	0.033	0.033	0.035
<i>wR</i> 2 (all data)	0.088	0.093	0.088	0.081
Max./min. diff. peak [e·Å ^{–3}]	0.31/–0.29	0.35/–0.42	0.29/–0.31	0.26/–0.32

point vibrational energies (ZPE) were calculated at the same level. All structures reported here are minima on the potential energy surface (only positive eigenvalues of the Hessian matrix). Population analyses were carried out with the NBO module^[23] included in the Gaussian 98 package. Due to problems with the handling of diffuse basis functions which occurred for some molecules in the NBO module, all population analyses were carried out using 6-31 g* wave functions with the molecular structures obtained at the 6-31(+)*g* level. Comparison of the results of NBO analyses using both a 6-31 g* or a full 6-31(+)*g* wave function was feasible for **2** and showed no significant differences between both approaches.

X-ray Crystallographic Study: Crystal structure determinations were carried out for **2**, **3**, **6**, **7**. All data were collected with a Nonius Kappa CCD diffractometer at -150°C using Mo- K_{α} radiation ($\lambda = 0.71073 \text{ \AA}$). The structures were solved by direct methods (SHELXS-97^[26]). The non-hydrogen atoms were refined anisotropically, H atoms were refined using a riding model [full-matrix least-squares refinement on F^2 (SHELXL-97^[27])]. Details of data collection and refinement are given in Table 6. A complete list of bond lengths and angles, thermal parameters, and positions of hydrogen atoms is available as Supporting Information. Crystallographic data (excluding structure factors) for the structures reported in this paper have been deposited with the Cambridge Crystallographic Data Centre as supplementary publications no. CCDC-161501 (**2**), -161502 (**3**), -161503 (**6**), -161504 (**7**). Copies of the data can be obtained free of charge on application to CCDC, 12 Union Road, Cambridge CB2 1EZ, UK [Fax: (internat.) + 44-1223/336-033; E-mail: deposit@ccdc.cam.ac.uk].

Acknowledgments

Financial support by the Deutsche Forschungsgemeinschaft is gratefully acknowledged.

- [1] A. Schmidpeter, M. Thiele, *Angew. Chem.* **1991**, *103*, 333; *Angew. Chem. Int. Ed. Engl.* **1991**, *30*, 308.
- [2] D. Gudat, V. Bajorat, M. Nieger, *Bull. Chim. Soc. Fr.* **1995**, *132*, 280.
- [3] D. Gudat, *Coord. Chem. Rev.* **1997**, *173*, 71.
- [4] D. Gudat, M. Schrott, V. Bajorat, M. Nieger, *Phosphorus Sulfur Silicon* **1996**, *109–110*, 125.
- [5] A. W. Holderberg, G. Schröder, D. Gudat, H.-P. Schröder, A. Schmidpeter, *Tetrahedron*. **2000**, *56*, 57.
- [6] D. Gudat, S. Hüp, M. Nieger, *Z. Anorg. Allg. Chem.*, in press.
- [7] See: K. B. Dillon, F. Mathey, J. F. Nixon, *Phosphorus: The Carbon Copy*, John Wiley, Chichester, **1998**, and references therein.
- [8] D. Gudat, V. Bajorat, S. Hüp, M. Nieger, G. Schröder, *Eur. J. Inorg. Chem.* **1999**, 1169.
- [9] B. Breit, *J. Mol. Catal. A* **1999**, *143*, 143.
- [10] B. Bogdanovic, in *Synthetic Methods of Organometallic and In-*

- organic Chemistry* (Ed.: W. A. Hermann), Georg Thieme Verlag, Stuttgart, **1996**, vol. 1, p. 46.
- [11] See for a preliminary account: D. Gudat, S. Hüp, L. Szarvas, M. Nieger, *Chem. Commun.* **2000**, 1637.
- [12] See: J. Tebby, *CRC Handbook of Phosphorus-31 Nuclear Magnetic Resonance Data*, CRC Press, Boca Raton, **1991**.
- [13] D. Gudat, M. Schrott, V. Bajorat, M. Nieger, *Phosphorus Sulfur Silicon* **1996**, *109–110*, 125.
- [14] S. O. Grim, J. H. Ambrus, *J. Org. Chem.* **1968**, *33*, 2993.
- [15] H. G. de Graaf, J. Dubbledam, H. Vermeer, F. Bickelhaupt, *Tetrahedron Lett.* **1973**, *9*, 2397.
- [16] D. Gudat, M. Nieger, M. Schrott, *Chem. Ber.* **1995**, *128*, 259.
- [17] B. F. Allen, O. Kennard, D. G. Watson, L. Brammer, A. G. Orpen, R. Taylor, in *International Tables for Crystallography* (Ed.: A. J. C. Wilson), Kluwer Academic Publishers, Dordrecht, **1992**, vol. C, p. 685pp.
- [18] J. C. Huffman, W. A. Skupinski, K. G. Caulton, *Cryst. Struct. Commun.* **1982**, *11*, 1435.
- [19] P. W. Coddling, K. A. Kerr, *Acta Crystallogr., Sect. B* **1978**, *34*, 3785.
- [20] A. D. Becke, *J. Chem. Phys.* **1993**, *93*, 5648.
- [21] M. J. Frisch, G. W. Trucks, H. B. Schlegel, G. E. Scuseria, M. A. Robb, J. R. Cheeseman, V. G. Zakrzewski, J. A. Montgomery, R. E. Stratmann, J. C. Burant, S. Dapprich, J. M. Millam, A. D. Daniels, K. N. Kudin, M. C. Strain, O. Farkas, J. Tomasi, V. Barone, M. Cossi, R. Cammi, B. Mennucci, C. Pomelli, C. Adamo, S. Clifford, J. Ochterski, G. A. Petersson, P. Y. Ayala, Q. Cui, K. Morokuma, D. K. Malick, A. D. Rabuck, K. Raghavachari, J. B. Foresman, J. Cioslowski, J. V. Ortiz, B. B. Stefanov, G. Liu, A. Liashenko, P. Piskorz, I. Komaromi, R. Gomperts, R. L. Martin, D. J. Fox, T. Keith, M. A. Al-Laham, C. Y. Peng, A. Nanayakkara, C. Gonzalez, M. Challacombe, P. M. W. Gill, B. G. Johnson, W. Chen, M. W. Wong, J. L. Andres, M. Head-Gordon, E. S. Replogle, J. A. Pople, *Gaussian 98 (Rev. A.7)*, Gaussian, Inc., Pittsburgh, PA, **1998**.
- [22] Neglect of counter-ions appeared justified considering that for both **1** and **5** experimental evidence suggested the absence of such interactions in both solution and the solid state; see refs.^[8,16]
- [23] [23a] J. P. Foster, F. Weinhold, *J. Am. Chem. Soc.* **1980**, *102*, 7211. — [23b] A. E. Reed, F. Weinhold, *J. Chem. Phys.* **1985**, *83*, 1736. — [23c] J. F. Carpenter, F. J. Weinhold, *J. Mol. Struct. (Theochem)* **1988**, *169*, 41.
- [24] It should be noted that the calculated orbitals are Kohn–Sham orbitals. As such, these are strongly dependent on the chosen functional but may still be used for a qualitative interpretation of chemical phenomena, as has been discussed by the groups of Baerends and Hoffmann: [24a] E. J. Baerends, O. V. Gritsenko, *J. Phys. Chem.* **1997**, *101*, 5383. — [24b] R. Stowasser, R. Hoffman, *J. Am. Chem. Soc.* **1999**, *121*, 3414.
- [25] Involvement of a continuous model treatment to the computed gas-phase structures revealed that the π -population are not affected by solvation effects. This suggests that the rating of the canonical contributions should be similar in the gas phase and in solution or the solid state.
- [26] SHELXS-97: G. M. Sheldrick, *Acta Crystallogr., Sect. A* **1990**, *46*, 467.
- [27] SHELXL-97: G. M. Sheldrick, University of Göttingen, **1997**.

Received April 9, 2001

[101128]